International Journal for Modern Trends in Science and Technology
Volume 9, Issue 10, pages 46-52.
ISSN: 2455-3778 online
Available online at: http://www.ijmtst.com/vol9issue10.html
DOI: https://doi.org/10.46501/IJMTST0910006

Path following control for four-wheel-drive/ four-wheel-steer mobile robot (4WD4WS) by front and rear independent driving method

Nam Kien Dang [1] | Vu Nguyen [2*]

[1]Researcher, Control, Automation in Production and Improvement of Technology Institute (CAPITI), Academy of Military Science and Technology (AMST), Hanoi, Vietnam.
dangnamkien@gmail.com
[2]Assistant Professor, Faculty of Electrical Engineering, Hanoi University of Industry, Hanoi, Vietnam.
vutudonghoa@yahoo.com.vn

To Cite this Article
Nam Kien Dang and Vu Nguyen. Path following control for four-wheel-drive/ four-wheel-steer mobile robot (4WD4WS) by front and rear independent driving method, International Journal for Modern Trends in Science and Technology, 2023, 9(10), pages. 46-52.https://doi.org/10.46501/IJMTST0910006

Article Info
Received: 16 October 2023; Accepted: 24 October 2023; Published: 25 October 2023.

ABSTRACT

The majority of traction studies for 4WD4WS active four-wheel-drive robots are conducted with the kinematics of simpler configurations, which reduce the robot's maneuverability and flexibility. This paper proposes a method of geometric dynamic control for the robot with the ability to better utilize the superior kinematics of the 4WD4WS robot, which is the independence of the front wheels from the rear wheels. The process of synthesizing control laws is strictly mathematically guaranteed. The simulation in Matlab shows the research results visually.

Keywords— mobile robot; path following; four-wheel-drive/four-wheel-steer; 4WD4WS, virtual target guidance algorithm.

1. INTRODUCTION

The four-wheel-independent-drive and four-wheel-independent-steer robot or 4WD4WS is a redundant drive system with outstanding flexibility and mobility with 8 motors (4 drive motors and 4 steering motors) is being used widely. In addition to its high road holding ability and performance, 4WD4WS is also used in harsh conditions such as agricultural tool vehicles.

In mobile robot control, the problem of robot tracking is a common problem, ensuring that the robot can be applied in practice. With 4WD4WS, some authors built the controller on a dynamic model with unrealistic assumptions about the system's responsiveness [9], when the robot, in fact, is a non-holonomic system despite the residual drive. [10] is one of the very detailed studies with the introduction of two separate control loops, in which the steering loop also provides independent forward and rear steering angles. However, by imposing the same steering angle on the front and

rear wheels [10, 11], the author has created a side slip angle at the drive wheels in all operating cases.

Some authors research geometric steering methods and Pure Pursuit is one of the most widely used and developed steering methods [3, 4, 5], but the application of 4WD4WS is not mentioned. There is also a virtual target aiming method [1, 2] applied with the 4WD4WS robot, however, binding the front and rear steering angles reduces the mobility and flexibility of the robot.

Currently, the popular application of image processing has brought many favorable results for control problems, including many studies using cameras and computer vision systems to determine object distances. [6, 7, 8]. Therefore, with the use of two cameras, one to determine the dynamic virtual aiming point, the other to determine the horizontal deviation of the vehicle body, the author proposes an independent steering method for the front and rear steering wheels in the bicycle model of 4WD4WS robot.

2. METHODOLOGY

A. The kinematicmodel of 4WD4WS mobile robot

A popular kinematic model for 4WD4WS robots used by many researchers is a simplified model of a two-wheeled bicycle. In which the steering angles of each real wheels as well as the virtual wheels F and R (as shown in Figure 1) are determined through the Ackermann steering method with the instantaneous center of rotation I_{CR}..

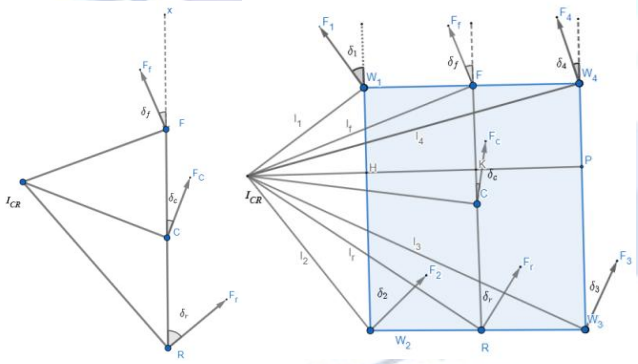

Fig. 1. The simplified two-wheeled bicycle kinematic model

$$\tan(\delta_f) = \frac{\frac{l}{2}+R*\sin(\delta_c)}{R*\cos(\delta_c)} \quad (1)$$

$$\tan(\delta_r) = \frac{-\frac{l}{2}+R*\sin(\delta_c)}{R*\cos(\delta_c)} \quad (2)$$

Where: $\delta_f, \delta_r, \delta_c$ are the virtual steering angles at points F, R, C; wheel base $l = 2 * l_f = 2 * l_r$, $d$is the vehicle width. R is the trajectory radius, as in fig. 1: $R = I_{CR}C$. $\delta_i, i = 1,2,3,4$are the real steering angles atreal wheels – angles between the longitudinal car axis and wheel planes.

Similarly, when considering right triangles IHW_1, IHW_2, IPW_3, IPW_4, we have the relations for each steering angle of the wheels:

$$\delta_1 = \tan^{-1}\frac{\frac{l}{2}+R*\sin(\delta_c)}{R*\cos(\delta_c)-\frac{d}{2}} \quad (3)$$

$$\delta_2 = \tan^{-1}\frac{-\frac{l}{2}+R*\sin(\delta_c)}{R*\cos(\delta_c)-\frac{d}{2}} \quad (4)$$

$$\delta_3 = \tan^{-1}\frac{-\frac{l}{2}+R*\sin(\delta_c)}{R*\cos(\delta_c)+\frac{d}{2}} \quad (5)$$

$$\delta_4 = \tan^{-1}\frac{\frac{l}{2}+R*\sin(\delta_c)}{R*\cos(\delta_c)+\frac{d}{2}} \quad (6)$$

So with given R and δ_c, we can completely rely on (1-6) to find all remaining steering angles of the vehicle.

On the contrary, if given $\delta_i, i = 1,2,3,4$, it is completely possible to find R and δ_c according to the equations below:

$$\delta_f = \tan^{-1}\frac{2}{\cot(\delta_1)+\cot(\delta_4)} \quad (7)$$

$$\delta_r = \tan^{-1}\frac{2}{\cot(\delta_2)+\cot(\delta_3)} \quad (8)$$

$$\delta_c = \tan^{-1}\frac{\tan(\delta_f)+\tan(\delta_r)}{2} \quad (9)$$

$$R = \frac{l}{\cos(\delta_c)*(\tan(\delta_f)-\tan(\delta_r))} \quad (10)$$

Meanwhile, with the assumption of driving according to the Ackermann method, friction forces will eliminate horizontal movements of the vehicle body and slipping will not occur, and the vehicle will move at a constant speed v. Then the angular velocity of the vehicle body is calculated by:

$$\dot{\psi} = \omega = \frac{v}{R} \quad (11)$$

Project the velocity vector v onto the two axes of the fixed ground coordinate system:

$$\begin{cases} \dot{x} = v\cos\psi \\ \dot{y} = v\sin\psi \end{cases} \quad (12)$$

Combining (9), (10), (11), (12) we get the kinematic equations of 4WD4WS:

$$\begin{cases} \dot{x} = v\cos\psi \\ \dot{y} = v\sin\psi \\ \dot{\psi} = \frac{v}{R} \\ R = \frac{l}{\cos(\delta_c)*(\tan(\delta_f)-\tan(\delta_r))} \\ \delta_c = \tan^{-1}\frac{\tan(\delta_f)+\tan(\delta_r)}{2} \end{cases} \quad (13)$$

With$\delta_f$andδ_r as control inputs.

B. Path following control for 4WD4WS by front and rear independent driving method

With 2 cameras and image processing unit placed on the vehicle body, it is possible to simultaneously determine the angle of deviation of the vehicle body (fixed front camera [2]) and the distance from the vehicle body to the required path. Then the front wheel steering angle δ_f is steered according to the dynamic virtual target method [2] while the rear wheel steering angle δ_r is steered according to the conventional virtual target method [1].

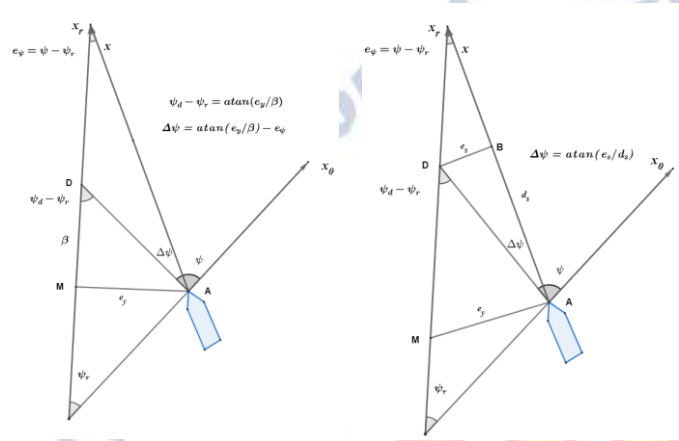

a, Conventional virtual target method b, Dynamic virtual target method

Fig 2. Two geometric steering methods

Figure 2 shows two steering methods, in which, as in [1] the goal of steering towards a normal virtual target point (Figure 2.a) is to aim at point D to steer by determining the angles as follows :

$$e_\psi = \psi - \psi_r \quad (14)$$

$$\psi_d - \psi_r = \text{atan}(\frac{e_y}{\beta}) \quad (15)$$

$$\Delta\psi = \psi_d - \psi_r - e_\psi = \text{atan}\left(\frac{e_y}{\beta}\right) - e_\psi \quad (16)$$

Thus, with β being a positive parameter (selecting the requirement for convergence speed as well as system responsiveness (maximum steering angle)), it is possible to determine the deflection angle $\Delta\psi$ necessary so that the robot follows the required trajectory when obtaining e_ψ and e_y values from cameras and image processing systems.

While Figure 2.b shows the dynamic virtual target steering method (as in [2]), the virtual target point D is determined and targeted by determining the deflection angle $\Delta\psi$ as follows:

$$\Delta\psi = \text{atan}\left(\frac{e_s}{d_s}\right) \quad (17)$$

Where e_s is the measured straight camera deviation compared to the required trajectory and d_s is the camera focal length (front view distance, a positive parameter selected based on trajectory curvature and vehicle speed).

The method of independent steering of the front and rear wheels is done in 2 steps, steering with dynamic virtual target points for both wheels and then steering the rear wheels with the conventional virtual target aiming method. Then similar to [2], we have the first system of equations:

$$\begin{cases} \Delta\dot{\psi} = 2\frac{v}{l}\tan\delta_f - \dot{\psi}_d \\ \dot{\delta_f} = \frac{K}{T}u_f - \frac{1}{T}\delta_f \end{cases} \quad (18)$$

By using Terminal sliding mode control [2], can find:

$$u_f = \frac{\delta_f}{K} - \frac{2\lambda vT}{Kl}\tan\delta_f + \frac{\lambda T}{K}\dot{\psi}_d - K_d s^{\frac{1}{n}} \quad (19)$$

From (13) we can achieve the second system equations, equivalent to the second step controlling the rear wheelindependently:

$$\begin{cases} \Delta\dot{\psi} = \frac{v}{l}\cos(\text{atan}(\frac{1}{2}(\tan\delta_f + \tan\delta_r))(\tan\delta_f - \tan\delta_r) - \dot{\psi}_d \\ \dot{\delta_r} = \frac{K}{T}u_r - \frac{1}{T}\delta_r \end{cases} \quad (20)$$

Considering δ_f as a parameter, the front and rear wheel controllers can use the same set of parameters (K,T).

From (16) one can get:

$$\text{atan}\left(\frac{e_y}{\beta}\right) - e_\psi = \Delta\dot{\psi}\tau + \Delta\psi_0 \quad (21)$$

With τ is them time to reach the desired angle $\Delta\psi$.

Then $\Delta\dot{\psi}_d$ can be calculated by:

$$\Delta\dot{\psi}_d = \frac{1}{\tau}(\text{atan}\left(\frac{e_y}{\beta}\right) - e_\psi - \Delta\psi_0) \quad (22)$$

Subtitue to (20) one can get:

$\cos(\text{atan}(\frac{1}{2}(\tan\delta_f + \tan\delta_{rd}))(\tan\delta_f - \tan\delta rd) = 1\tau\text{atan}ey\beta - e\psi - \Delta\psi 0 + \psi dlv$ (23)

Set $K_x = \frac{\left[\frac{1}{\tau}\left(\text{atan}\left(\frac{e_y}{\beta}\right) - e_\psi - \Delta\psi_0\right) + \dot{\psi}_d\right]l}{v}$ as a calculable parameter when assuming $\dot{\psi}_d$ as a bounded noise.

Then (23) can be rewritten:

$\cos(\text{atan}(\frac{1}{2}(\tan\delta_f + \tan\delta_{rd}))(\tan\delta_f - \tan\delta rd) = Kx$ (24)

Where $0 < cos(atan(\frac{1}{2}(\tan\delta_f + \tan\delta_{rd})) \leq 1$ so:

$$(\tan\delta_f - \tan\delta_{rd}) \geq K_x \quad (25)$$

Ortan $\delta_{rd} \leq \tan\delta_f - K_x$ with the range of steering angles $(-\pi/4, \pi/4)$ one can have :

$$\delta_{rd} \leq \text{atan}(\tan\delta_f - K_x) \quad (26)$$

When in this independent steering method:

$$\delta_r = \alpha - \delta_f \quad (27)$$

where$\alpha$is the independent partand always have the opposite sign from$\delta_f$or$\alpha = -K_\alpha \delta_f$with$K_\alpha$positive.

Combine (26) with (27):

$$\alpha \leq \text{atan}(\tan \delta_f - K_x) + \delta_f \quad (28)$$

Then one can find:

$$\delta_{rd} = -(K_\alpha + 1)\delta_f \quad (29)$$

Equation (29) is ensured when $\delta_f = 0$then$\delta_{rd} = 0$.

Similarly to [1] u_r can be found:

$$u_r = K_r(\delta_{rd} - \delta_r) + \dot{\delta}_{rd} \quad (30)$$

Thus, the control input values of both the front and rear wheels can be determined explicitly, serving as the basis for building simultaneous and independent controllers of the front and rear wheels.

C. Simulations

The article chooses to simulate a circular trajectory with 3 radii corresponding to: 20 m, 50 m, 100 m, then the forward viewing distance of the camera is corresponding to 2 m, 5 m, 5 m. While the moving speed of the robot car is 2 m/s. The simulation results will be compared with the dynamic virtual target steering method mentioned in [2].

3. RESULTS AND DISCUSSION

Simulation results on Matlab Simulink software are shown in Fig. 3 to Fig. 8. In particular, it can be seen that the lateral error of the vehicle body has been significantly improved when comparing the proposed control method with dynamic virtual target method. When the trajectory radius is 20 m, with the independent steering method the lateral error is about 5* 10-5 m while the error with the dynamic virtual target method under the same conditions is 2.5* 10-4 m. When the trajectory radius is 50 m and the look forward distance increases to 5 m, the trajectory tracking error of the two methods is 5* 10-3 m and 0.15 m, respectively. When the trajectory radius increases to 100 m, the trajectory tracking error is 2.9* 10-3 m and 0.075 m, respectively.

However, the trajectory tracking of the dynamic virtual target method is smoother, without much fluctuation around the balance value. With the ability to customize the parameters of the rear wheel, this drawback actually represents an advantage of the independent steering method: being able to customize the parameters to choose between trajectory tracking error and trajectory smoothness.

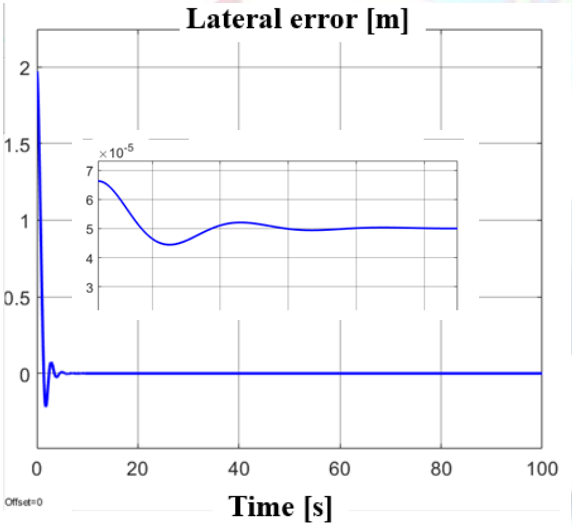

Fig.3 Lateral error of independent steering method of front and rear wheels when trajectory radius is 20 m

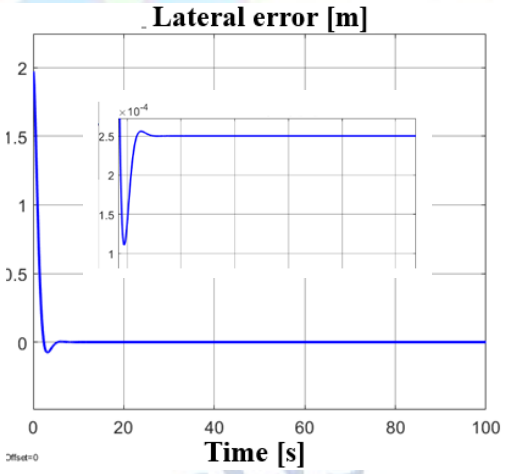

Fig. 4. Lateral error of dynamic virtual target steering method when trajectory radius is 20 m

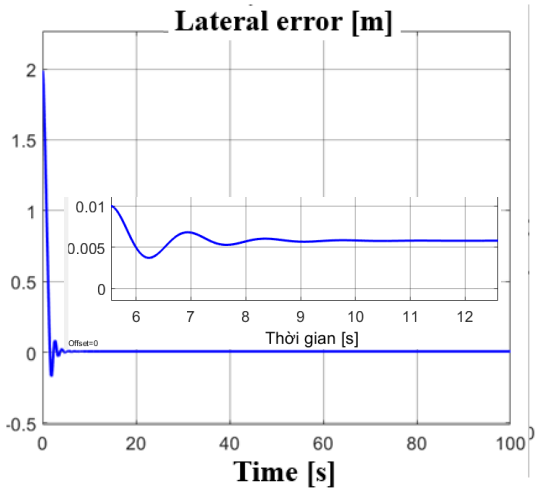

Fig.5Lateral error of independent steering method of front and rear wheels when trajectory radius is 50 m

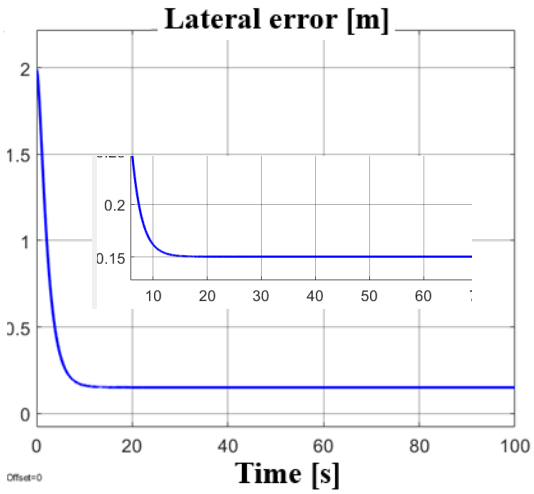

Fig.6. Lateral error of dynamic virtual target steering method when trajectory radius is 50 m

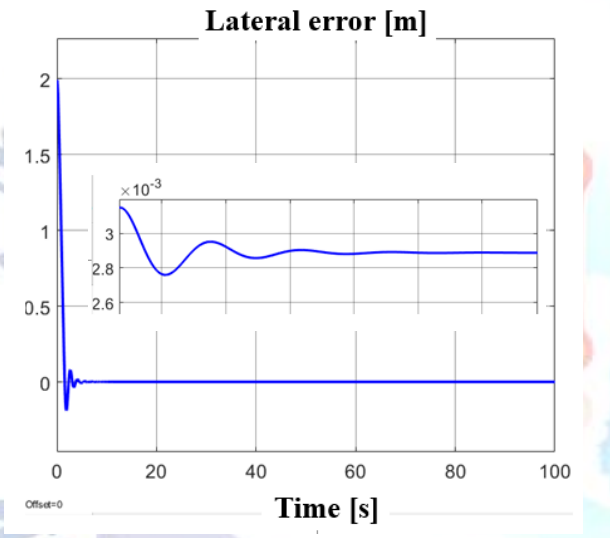

Fig.7Lateral error of independent steering method of front and rear wheels when trajectory radius is 100 m

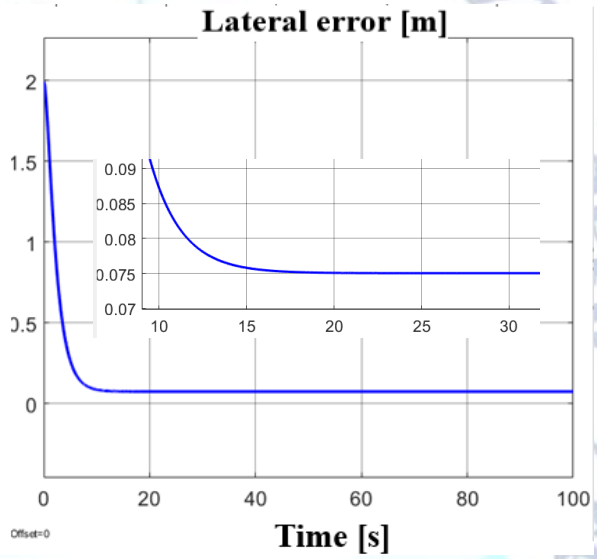

Fig.8. Lateral error of dynamic virtual target steering method when trajectory radius is 100 m

Parameter choices can be made as shown in Fig. 9 to Fig. 14.

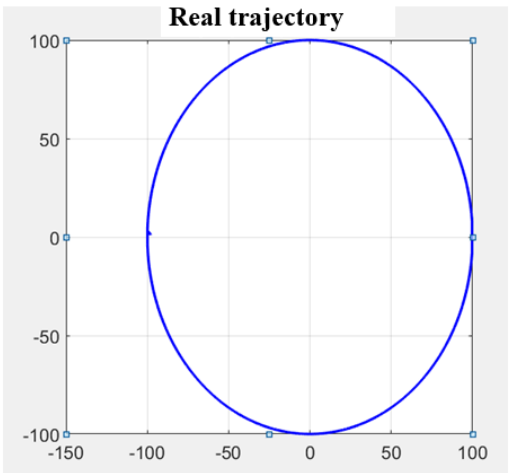

Fig. 9. Actual trajectory of the vehicle when following a 100 m radius trajectory with$\beta = 0.1$

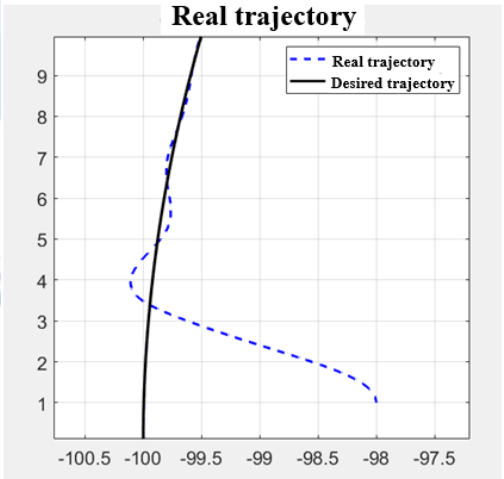

Fig. 10. Comparison of the actual trajectory with the required trajectory when the trajectory radius is 100 m with$\beta = 0.1$

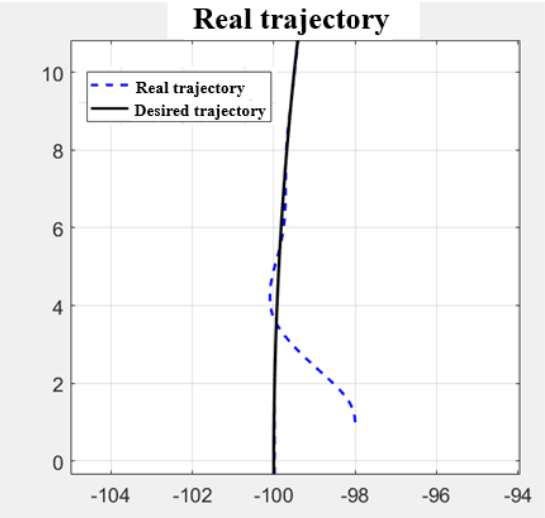

Fig. 11. Comparison of the actual trajectory with the required trajectory when the trajectory radius is 100 m with$\beta = 0.2$

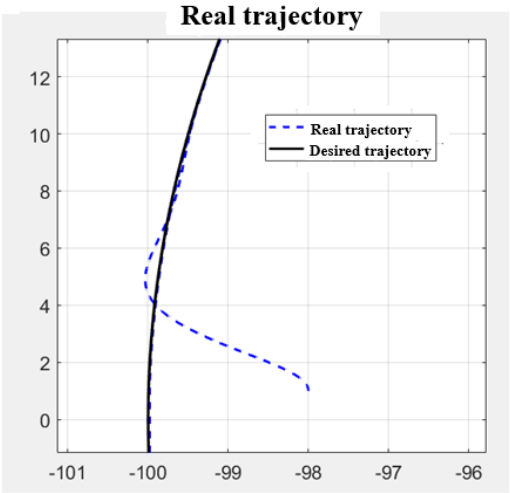

Fig. 12. Comparison of the actual trajectory with the required trajectory when the trajectory radius is 100 m with$\beta = 0.5$

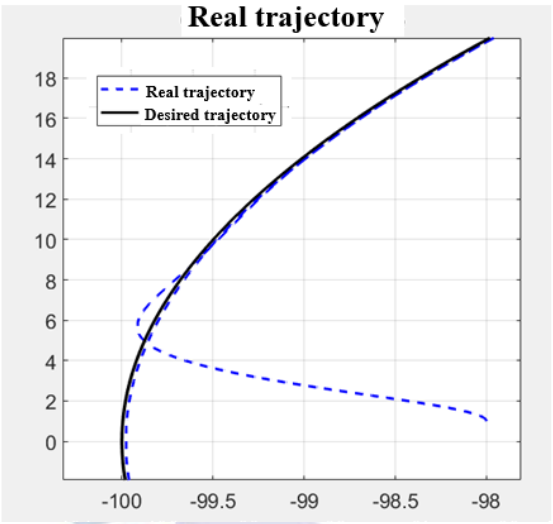

Fig. 13. Comparison of the actual trajectory with the required trajectory when the trajectory radius is 100 m with$\beta = 1$

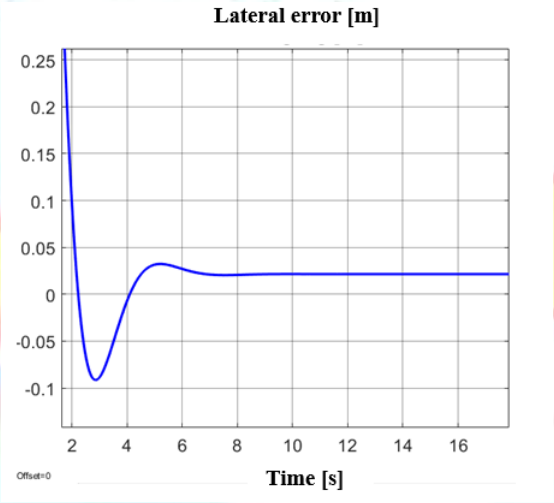

Fig. 14. Lateral errorwhen the trajectory radius is 100 m with$\beta = 1$

4. CONCLUSIONS

The article has presented an algorithm to independently control the front and rear wheels considering the problem of trajectory tracking for 4WD4WS mobile robot, whereby the quality of trajectory tracking is improved compared to other available solutions, while ensuring the mobility and flexibility of the residual driving robot. With that result, this method can be applied to other wheeled mobile robots with similar kinematic configurations, ensuring high efficiency. Research results are rigorously mathematically proven and visualized by simulation.

Conflict of interest statement

Authors declare that they do not have any conflict of interest.

REFERENCES

[1]. Nam Kien Dang , Vu Nguyen, Thanh Trung Nguyen, "*Path following calibration for four-wheel-drive/four-wheel-steer mobile robot (4WD4WS) by referrence objects.*", Journal of Military Science and Technology, Vol. 85 (02-2023).

[2]. Nam Kien Dang , Vu Nguyen, Dynamic virtual target guidance algorithm for path following control of a 4WD4WS mobile robot, International Journal of Multidisciplinary Research and Growth Evaluation, E-ISSN 2582-7138, 2023, Vol. 4, Issue. 4, pp. 896-902, DOI: https://doi.org/10.54660/.IJMRGE.2023.4.4.896-902

[3]. Zhao Z.G., Zhou L.J., Zhu Q., Preview Distance Adaptive Optimization for the Path Tracking Control of Unmanned

Vehicle, J. Mech. Eng.. 54 (24) (2018) 180–187, 10.3901/JME.2018.24.166.

[4]. H. Wang, X. Chen, Y. Chen, B. Li and Z. Miao, "Trajectory Tracking and Speed Control of Cleaning Vehicle Based on Improved Pure Pursuit Algorithm," 2019 Chinese Control Conference (CCC), Guangzhou, China, 2019, pp. 4348-4353, doi: 10.23919/ChiCC.2019.8865255

[5]. W. J. Wang, T. M. Hsu and T. S. Wu, "The improved pure pursuit algorithm for autonomous driving advanced system," 2017 IEEE 10th International Workshop on Computational Intelligence and Applications (IWCIA), Hiroshima, Japan, 2017, pp. 33-38, doi: 10.1109/IWCIA.2017.8203557.

[6]. S. V. F. Barreto, R. E. Sant'Anna and M. A. F. Feitosa, "A method for image processing and distance measuring based on laser distance triangulation," 2013 IEEE 20th International Conference on Electronics, Circuits, and Systems (ICECS), Abu Dhabi, United Arab Emirates, 2013, pp. 695-698, doi: 10.1109/ICECS.2013.6815509.

[7]. Ming-Chih Lu, Wei-Yen Wang and Chun-Yen Chu, "Image-based distance and area measuring systems," in IEEE Sensors Journal, vol. 6, no. 2, pp. 495-503, April 2006, doi: 10.1109/JSEN.2005.858434.

[8]. Chen-Chien Hsu, Ming-Chih Lu and Ke-Wei Chin, "Distance measurement based on pixel variation of CCD images," 2009 4th International Conference on Autonomous Robots and Agents, Wellington, New Zealand, 2009, pp. 324-329, doi: 10.1109/ICARA.2000.4803985.

[9]. Lee Ming-Han and Tzuu-Hseng S. Li. “Kinematics, dynamics and control design of 4WIS4WID mobile robots.” The Journal of Engineering 2015 (2015): 6-16.

[10]. Penglei Dai & Jay Katupitiya (2018) Force control for path following of a 4WS4WD vehicle by the integration of PSO and SMC, Vehicle System Dynamics, 56:11, 1682-1716, DOI: 10.1080/00423114.2018.1435888.

[11]. Zhonghua Zhang, Caijin Yang, Weihua Zhang, Yanhai Xu, Yiqiang Peng, Maoru Chi, "Motion Control of a 4WS4WD Path-Following Vehicle: Dynamics-Based Steering and Driving Models", Shock and Vibration, vol. 2021, Article ID 8861159, 13 pages, 2021. https://doi.org/10.1155/2021/8861159.